Available online at www.sciencedirect.com
SCIENCE DIRECT
Surface & Coatings Technology 192 (2005) 19–26
SURFACE & COATINGS TECHNOLOGY
www.elsevier.com/locate/surfcoat

Structural study of iron-based microstructured and nanostructured powders sprayed by HVOF thermal spraying

M. Cherigui*, N.E. Fenineche, C. Coddet

Laboratoire d'Etudes et de Recherches sur les Matériaux, les Plasmas et les Surfaces (LERMPS), Université de Technologie de Belfort-Montbéliard (UTBM), Site de Sévenans, Belfort Cedex 90 010, France

Received 19 December 2003; accepted in revised form 20 February 2004
Available online 27 April 2004

Abstract

The paper deals with the structure and magnetic properties of coatings obtained by HVOF spraying using microcrystalline and nanocrystalline powders.

For FeNb coatings sprayed using microcrystalline powders, X-ray diffraction showed partially amorphous structure. For FeSi ones, the structure was completely crystalline.

For FeSi coatings sprayed using nanocrystalline powders, X-ray diffraction showed the crystalline size was lower than that in the coating obtained from microcrystalline powder. For FeSiB alloys, the structure is crystalline with a small quantity of amorphous phase. FeSi coatings behaved as a soft ferromagnetic. On other hand, the FeSiB coatings presented.

Keywords: Amorphous; High velocity oxyfuel (HVOF); Iron alloy; Magnetic properties

1. Introduction

Nanomaterials (<100 nm grain sizes) are in the early stage of development but show already many interesting properties and advantages over conventional coarse counterparts [1].

As far as the magnetic properties are concerned some fine crystal exhibit good hard magnetic properties [2]. Recently, it became obvious that nanosized materials also have good soft magnetic properties [3]. Indeed, soft magnetic alloys having extraordinary magnetic properties can be realized by establishing nanometer grain structure [4]. An important issue now concerns to fabricate massive nanocrystalline parts with this regard several processing routes are being developed [3,4]. In particular, the processing of nanocrystalline coatings by thermal spray has been recently successfully achieved for Ni and Fe based alloys [5,6]. The major advantage of this processing route is its cost effectiveness compared at rapid quenching or mechanical alloyed methods, which may rapidly lead to industrial application of nanocrystalline materials.

A significant number of alloys are likely to have a noncrystalline structure (amorphous or pseudo amorphous) when they are solidified at a speed higher than 10^5 °C/s.

Iron silicides are used as starting material for many multicomponent technical alloys. For example, $\beta FeSi_2$ and Fe_2Si_5 alloys with a Cu are considered as attractive materials for high temperature thermoelectric applications [7,8].

Generally, for the FeSi alloys, the saturation magnetization decreases with increasing Si content. However, the specific resistance increases and the magnetocrystallinity decreases at the same time.

FeNb alloy was chosen as feedstock material for its good tendency to form amorphous phase [9–11]. Literature is very poor on the use of such material as a feedstock for thermal spraying.

The choice of FeSiB is justified by the thermal stability of the residual amorphous phase enriched in boron and the good magnetic properties related to the presence of silicon where the boron increases the possibility of having an amorphisation of alloys [12]. Moreover, FeSiB amorphous have been widely used as a magnetic core material used in electric generator construction [13–15].

Although extensive studies have been reported on both irreversible and reversible structural relaxation in amor-

* Corresponding author. Tel.: +33-3-84-58-32-43; fax: +33-3-84-58-32-86.
E-mail address: mohamed.cherigui@utbm.fr (M. Cherigui).

0257-8972/$ - see front matter © 2004 Elsevier B.V. All rights reserved.
doi:10.1016/j.surfcoat.2004.02.023

phous magnetic alloys [16,17], very few studies have been made on FeBSi amorphous alloys in spite of the importance of its applications as magnetic materials [18].

There is a lot of techniques to produce amorphous alloys other than rapid quenching, namely vapour condensation on cold substrate, cathode sputtering, ion bombardments and electrolysis methods [19]. Thermal spraying has become a very advantageous method owing to the high deposition rates [20,21].

Thermal spraying process permits the use of various geometry substrates. Then its use is extended to a wide range of applications [18].

Nanocrystalline coatings obtained by thermal spraying exhibit different physical and mechanical attributes than those of microcrystalline coatings of comparable composition.

2. Experimental

2.1. Feedstock powders

In this study, two types of powders were used. For the microcrystallines powders, Fe–6.5 at.% Si and Fe–67.2 at.% Nb alloys with average granulometry sizes of 40 and 25 μm, respectively, were employed.

Concerning the nosized powders, FeSi and elemental Fe, Si and B powders, with an average particle size of 65, 30, 20 and 10 μm, respectively, were used in order to produce Fe–6.5 at.% Si and Fe–6.5at.% Si–18.5 at.% B nanostructured powder using the mechanical alloying during 48 h. The ball milling was carried out using a planetary high-energy ball milling (Retsch PM 400). Steel balls (diameter: 20 mm) and 50 ml volume jar were used. Four jars are mounted on a planar disc. With the rotation of the disc, the vials move in a circular and opposite direction compared to the disc rotation. The rotation speed of disc was equal to 400 rpm and the rotation speed of jar was equal to 800 rpm.

Resulting powders had granulometry sizes in the range of 45 and 40 μm for FeSiB and FeSi, respectively. Their grain sizes were estimated X-ray using diffraction with the Scherrer formula. They are about 10–12 nm for FeSiB and FeSi, respectively.

The choice of Si and B percentages in FeSiB alloy was based on results of the previous paper [11]. Indeed, one has found that the structure of FeNb coatings obtained by HVOF spraying is partially amorphous. FeNb alloy is used as a reference material to initiate a structural and electronic study of crystalline $Fe_{3-x}SiB_x$ and FeNb alloys via first principle total energy simulation method. The supercell approach was used to examine the local effect of boron atoms in the FeSi structure, and to compare the appropriate properties to those of FeNb alloy.

The electronic density of state (DOS) using the modified tetrahedron method of Blöchl et al. [22] was calculated. Our numerical calculations were carried using the Full Potential Linear Augmented Plane Wave (FPLAPW), a first principle total energy Density Functional Theory (DFT) based method. We used the scalar relativistic version without spin orbit coupling [23] as embodied in the wien2k code [24] which is thought to be from the most accurate implementations of the FPLAPW methods for the computation of the electronic structure of solids within density functional theory. In the FPLAPW method, the crystal unit cell is divided into two parts: atomic spheres centered on the atomic sites and an interstitial region. Inside the atomic spheres, the basis set used to describe electronic states employs atomic like functions, while in the interstitial region plane waves are used. Exchange and correlation effects were treated using the generalized gradient approximation (GGA) as described by Perdew et al. [25,26].

2.2. Coating preparation

Thermal spraying of the reconstituted granules was carried out using a "CDS 8944" HVOF gun. In this work methane was used as a fuel gas with nitrogen. This latter was used as a powder carrier gas. The coating was deposited into copper sheet having sizes 70×25×0.8 mm up to the thickness of about 200 μm. Substrate sheets were mounted on a cylindrical holder rotated at 245 rpm. The HVOF gun was placed in front of the substrates at a stand-off distance of 200 and 300 mm, to give a horizontal spray jet, and traversed vertically with a speed of 0.05 m s^{-1}. Spray parameters are showed in Table 1.

2.3. Deposit characterization

In order to determine the structural state of the phase present, X-ray diffraction was performed at a scanning rate of 3° per minute on samples of the as-received powder and as-sprayed coatings using monochromatic Cu-Kα radiation with a Philips X'Pert diffractometer. Samples were sectioned, polished and characterized using optical microscopy. Porosity content of freestanding coatings (3–4 mm wide and 10 mm long) was calculated using image analysis with

Table 1
Spraying parameters

Parameters	Microcrystalline powder	Nanocrystalline powder
Methane fuel flow rate (SLPM)	145	140
Oxygen gas flow rate (SLPM)	350	420
Oxygen rate in the mixture [Fuel/O_2] (vol.%)	0,41	0,33
Nitrogen carrier gas flow rate (SLPM)	20	20
Powder feed rate (g min^{-1})	35	35
Spray distance (mm)	250	300
Torch-Substrate relative velocity (m min^{-1})	245	245
Scanning velocity (mm s^{-1})	50	50
Deposit thickness (μm)	200	200

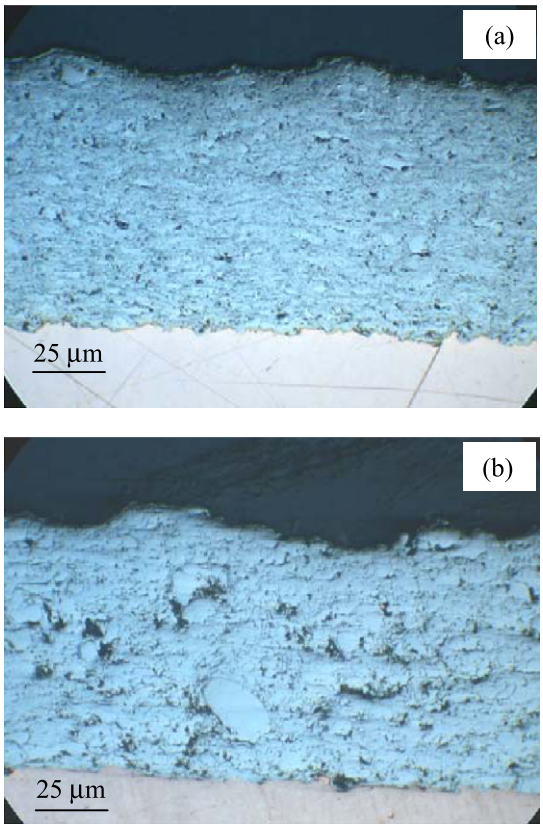

Fig. 1. Morphology of coatings: (a) FeNb, (b) FeSi (microcrystalline powders).

NIH image free software. The resulting data were average of six measurements.

Magnetic measurements were realized using a hysteresismeter Bull M2000 SIIS, which enabled to draw the hysteresis loop of the considered samples. It permitted also to measure magnetic properties, namely coercivity and saturation magnetization.

3. Results and discussion

3.1. Microcrystalline powders

The cross-section of the microstructured FeSi and FeNb coatings analyzed via optical microscopy is shown in Fig. 1. It is noticed that the coatings is dense, with the presence of porosity. The coating–substrate interface shows no gaps or cracks, which are characteristic features of good adhesion between the coating and the substrate.

Table 2
Porosities of FeNb, FeSi and FeSiB alloys

Alloys	Porosity (%)
FeNb (microcrystalline powder)	4±1.1
FeSi (microcrystalline powder)	8±2
FeSi (nanocrystalline powder)	4.5±1
FeSiB (nanocrystalline powder)	3.5±1

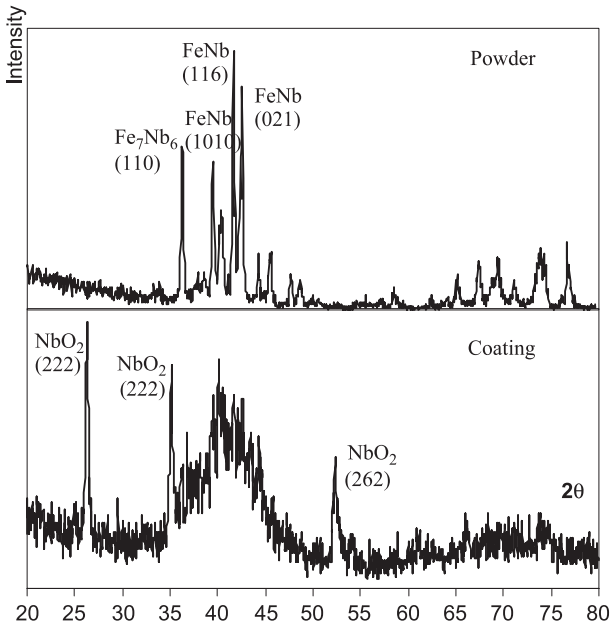

Fig. 2. X-rays diffraction of FeNb.

Observing the optical micrograph, the substrate surface is very irregular forming a favourable entry path of melted particles. The coating totally fills this entry path and follows exactly this extremely irregular surface. This is probably associated with the supersonic velocities of impact presented by the sprayed particles [27].

Table 2 summarizes porosities values of the two alloys.

Moreover, we can observe clearly that FeSi structure presents many pores which are favorable ways for oxygen to

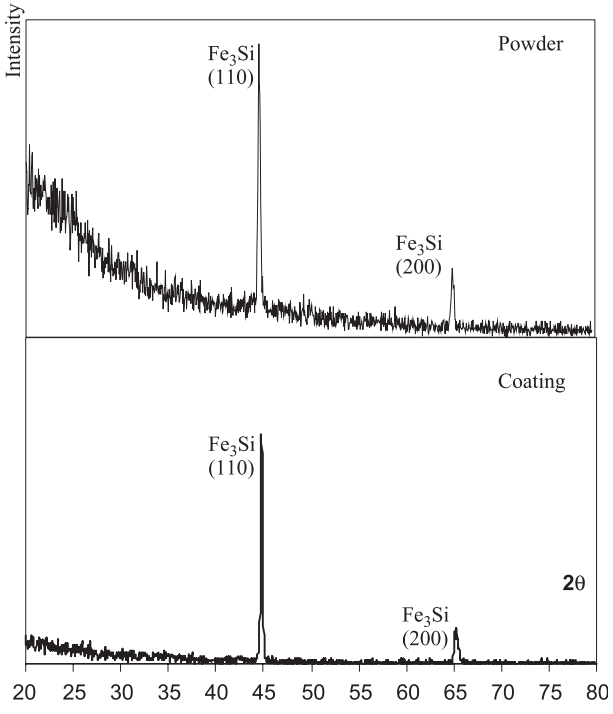

Fig. 3. X-rays diffraction of FeSi (microcrystalline powder).

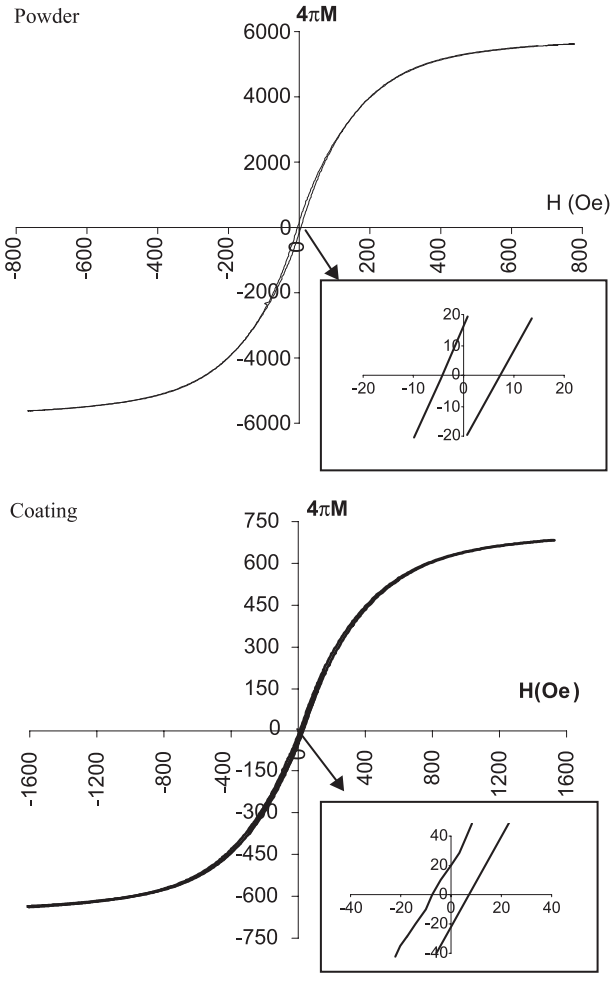

Fig. 4. Hysteresis loops for FeSi (microcrystalline powder).

enter in the latter easily and to form oxides. In addition, we can notice the presence of several non-molten particles in the deposit of FeSi as show in Fig. 1.

Fig. 2 shows the XRD patterns for FeNb coatings and powder. We can notice that the structure of the coatings is partially amorphous. We have also noted that the coatings have a FeNb structure with the presence of some oxides of NbO_2. These oxides result from the use of the HVOF process where phenomena of oxidation are less important comparing to APS process [11].

However, for FeSi alloy, the X-ray patterns showed that coatings structure is more crystallized than powder structure and that the cubic structure Fe_3Si is the principal characteristic for the FeSi alloy (Fig. 3). These results are similar to those obtained by rapid quenching of $Fe_{100-x}Si_x$ alloys [28] and FeSi mechanically alloys [29].

Concerning magnetic properties, the characterization did not enable to obtain Hysteresis loop of FeNb powder and coating because they have a superparamagnetic character. This result can be explained by the decrease of the average magnetic moment of FeNb alloy and the local magnetic moments with the Nb increasing concentration. The Nb has a local magnetic moment antiparallel to the Fe moment. The local magnetic moments of Nb and Fe hardly decrease, although the local magnetic moment of the alloy decreases significantly due to the antiparallel coupling [30].

A heat treatment of recrystallization at 800 °C during 20 min was carried out on the FeNb deposit. After this treatment, we have noted a value of the coercivity Hc of about 138 Oe.

Fig. 4 shows the hysteresis loops of the powder and the deposit for FeSi alloy. We can notice that the alloy is a soft ferromagnetic with an average coercivity Hc of 4 and 5 Oe for the powder and the coating, respectively.

3.2. Calculation details

Fig. 5 shows the electronic density of state (DOS) of Fe_3Si and FeNb alloys. The difference $E-E_{Fermi}$ is represented on the curves and the zero represents the Fermi level. The DOS histograms show the bonding state orbital near the Fermi level and the top of the density curve with the antibonding states.

The major difference that we can assert is the presence in the Fe_3Si histogram of a minimum of density just beyond the Fermi level, separating the peak of the antibonding states, whereas for the FeNb, the Fermi level is directly

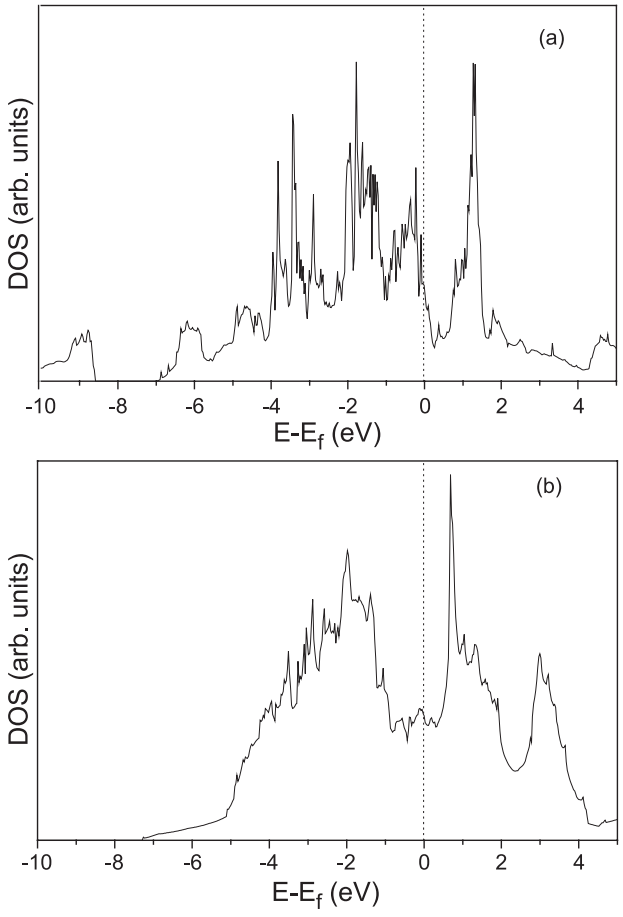

Fig. 5. Electronic density of state of Fe_3Si (a) and FeNb (b).

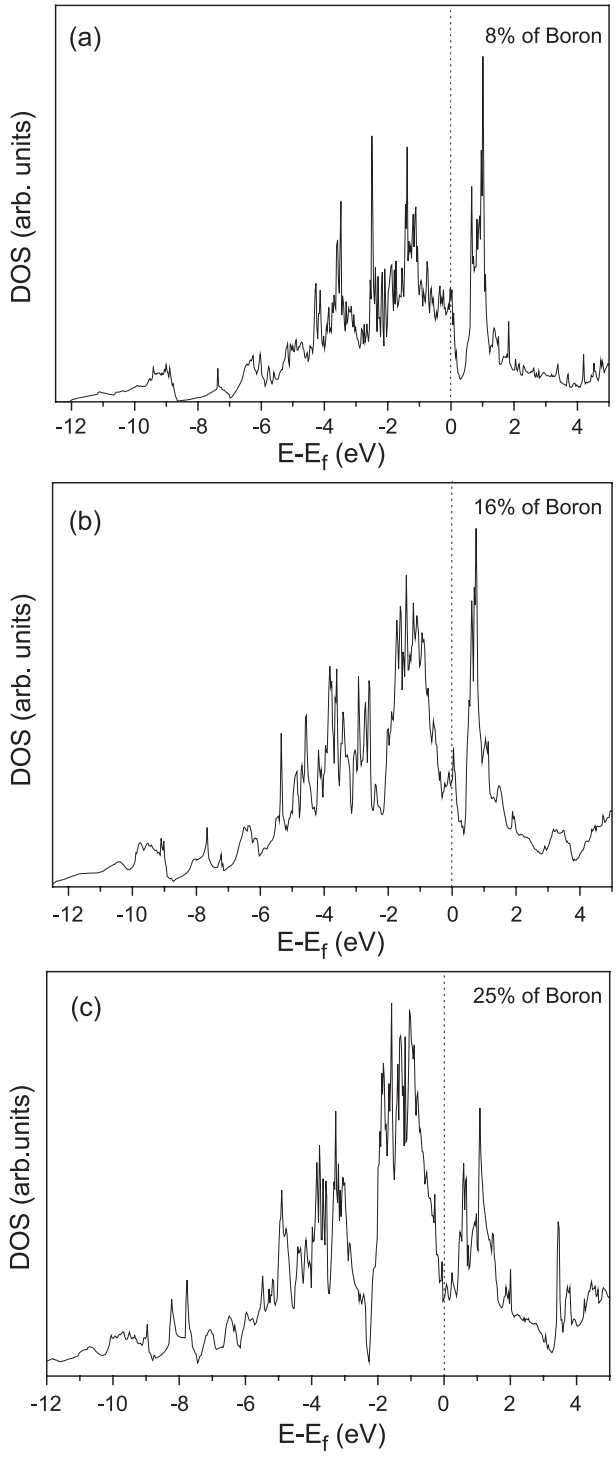

Fig. 6. Electronic density of state of boron-doped Fe_3Si alloy (a–c).

followed by a pronounced peak. In both compounds, the antibonding states are the localized d states: 4d-states from iron atoms in both cases, and 3d-states from niobium atoms in the second.

Another difference is that the peak of the lower energy part of the DOS present for Fe_3Si and which is due mainly to the tightly bounded s states is not visibly separated from the remaining parts of the DOS for the FeNb alloy. Accordingly, at finite temperatures, the antibonding states are much more populated in the case of FeNb alloy. The minimum of density beyond the Fermi level separating the bonding from the antibonding states in the Fe_3Si alloy denotes its structural stability.

On Fig. 6, density of state of B-doped Fe_3Si a, b and c correspond respectively to 8%, 16% and 25% of boron in the matrix are presented. It is noticed that the shape of DOS histogram is different: the addition of boron atoms annihilate gradually the minimum present near the Fermi level. In fact, this minimum is slightly reduced when the boron concentration is of 4%, and is less pronounced for 16% and disappears for 25% of boron. At the same time, the peak present in the bonding state is progressively pronounced, especially at the Fermi level, the density grows with increasing boron concentration. This is in conformity with the calculated values of bulk modulus, these later increases with the amount of boron, as shown in Fig. 7.

The fact that the antibonding states are more populated suggests that the addition of boron weaken the crystalline structure stability, even it reinforces the bonds as stated by the increasing bulk modulus. Furthermore, the lowest energy states are progressively connected with the remainder part of the histogram. Both changes make the electronic density of state similar to the FeNb one. Therefore, the bonding nature in the FeSiB alloy tends to have the same behavior than that of the niobium iron alloy due to the presence of boron.

3.3. Nanocrystalline powders

Based on a previous experience using a single parameter variation, the most significant spray parameters were adjusted to minimize the oxygen content as well as the porosity of the coatings.

Fig. 8a,b shows a cross-section from a dense coating FeSi and FeSiB, respectively.

Denser coatings were obtained for FeSiB coatings in comparison to FeSi deposits. However, FeSi structure

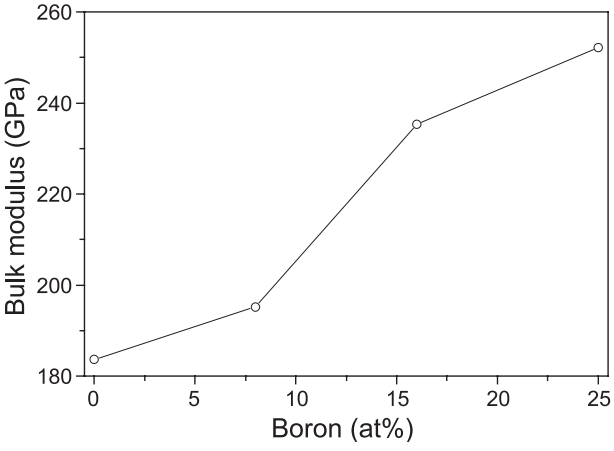

Fig. 7. Variation of bulk modulus values with boron content.

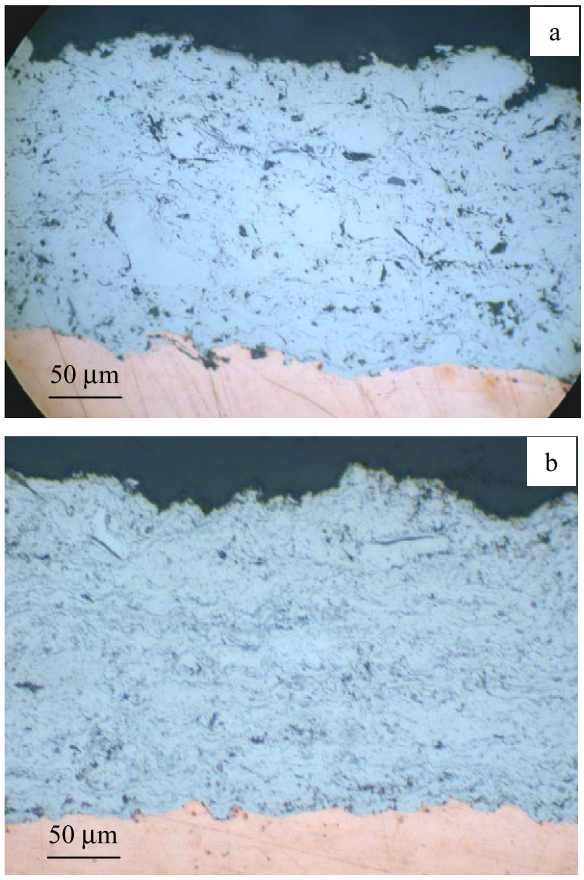

Fig. 8. Morphology of coatings: (a) FeSi, (b) FeSiB (nanocrystalline powders).

presents many pores, which are favorable ways for oxygen to enter in the latter easily and to form oxides. In addition, the presence of several non-molten particles in the FeSi deposit is clearly observed as shown in Fig. 8.

Table 2 summarizes the porosites of the two alloys.

Fig. 9 shows the X-ray diffraction of FeSi milled powder and coating. The diffraction peaks from the milled powder broaden noticeably, and their intensities decrease drastically. This indicates a significant change in the structure of the powder as a result of milling due to the decrease of crystallite size and increasing of atomic level strains.

These XRD patterns reveal the basically cubic structure α_1-Fe_3Si (DO_3) which is characteristic for the low silicon content FeSi alloys. These results agree with those obtained for rapidly quenched $Fe_{100-x}Si_x$ alloys [28] and mechanically alloyed FeSi [29].

Concerning FeSiB powder, it has noticed that the XRD patterns spectrum is similar to that of FeSi with the presence of a small amorphous phase percentage. These peaks are broader and the grain size is about 10 nm (Fig. 10). For FeSiB coating, it can be noted the presence of the same peaks of Fe_3Si with the presence of light amorphous phase percentage (Fig. 10). These results show that a variation of boron quantity in FeSiB alloys can increase the amorphous phase quantity in the coating.

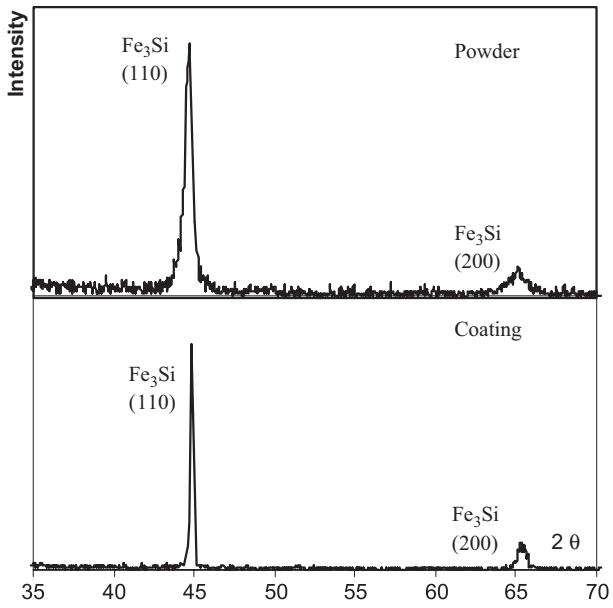

Fig. 9. X-ray diffraction patterns of FeSi (nanocrystalline powder).

Fig. 11 presents hysteresis loops of the FeSi mechanically alloyed powder after 48 h milling and thermal spraying coating, respectively. Soft magnetic character was recorded for FeSi ball milled powder. The coercivity value is about 0.28 Oe. However, FeSi coating showed coercivity Hc of about 15 Oe.

Usually the Hc values of for FeSi alloys (polycrystal or single crystal in the bulk) are less than about 1 Oe [31], while the obtained nanocrystalline FeSi alloys are more than about 100 Oe [32].

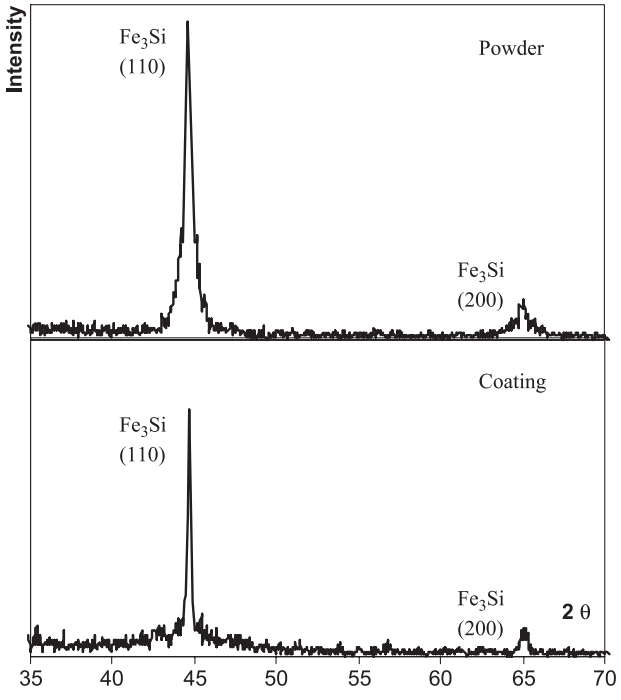

Fig. 10. X-ray diffraction patterns of FeSiB.

Generally, the Hc values of single-domain particles are much larger than those of the corresponding polycrystal and single crystal [32].

Other studies found for the same powder was an Hc value of about 0.025 Oe [32].

In the case of FeSiB, an increase in the coercivity values for powder and coating can be observed. Fig. 12 shows the hysteresis loops of FeSiB powder and coating. Hc values of about 17 and 26 Oe for the powder and coating respectively are registered.

The magnetization phenomenon is based on the displacement of the domain walls. For many materials, the domain walls move reversibly in very weak applied fields, while in stronger fields their motion becomes irreversible. Meanwhile, do not return to their original position when the magnetic field is removed.

The mean reason for this phenomenon is that the energy of the domain walls is not constant, but rather varies in an irregular mannes due to inhomogeneities in the specimen. These inhomogeneities which cause fluctuations of the wall energy are inclusions, second phases, dislocations, grain boundaries, internal stresses, group of point defects or impurity atoms, voids, etc. [33].

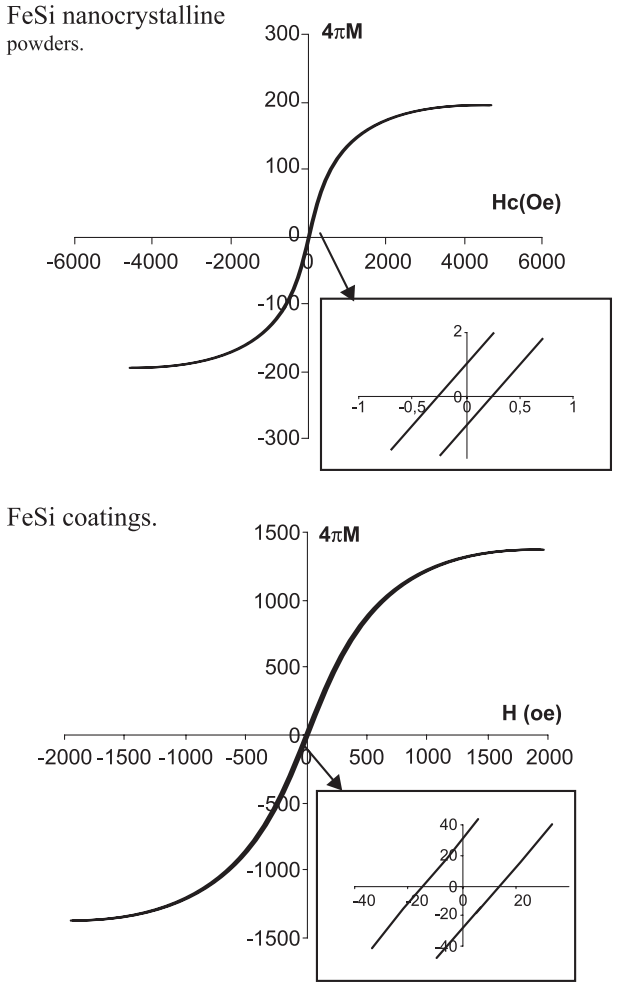

Fig. 11. Hysteresis loops of FeSi (nanocrystalline powder).

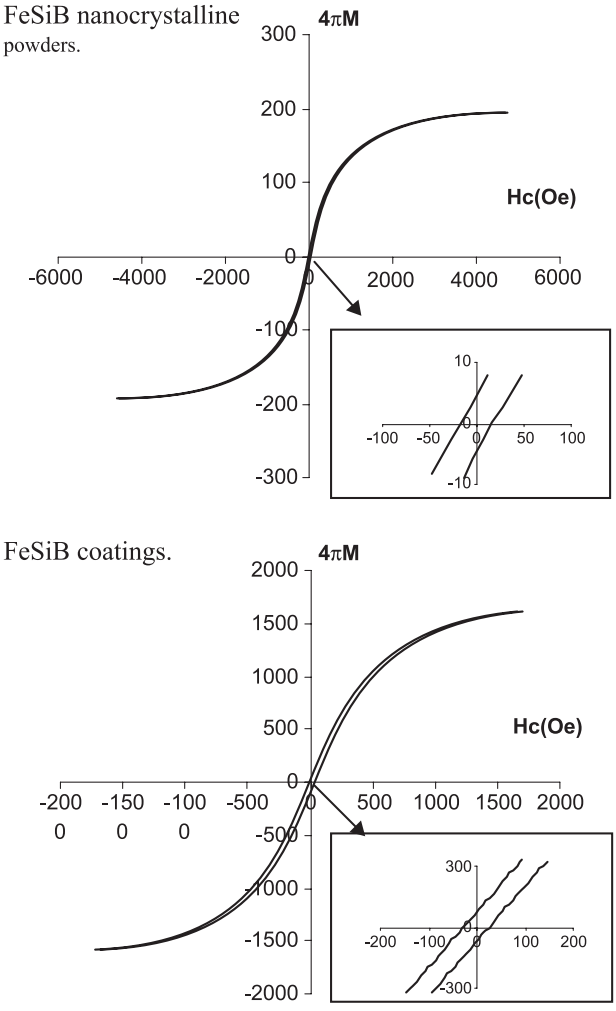

Fig. 12. Hysteresis loops of FeSiB.

In FeSiB alloys, boron additions in low amounts as nonmagnetic inclusions affect the magnetic structure by forming closing domains contributing to wall anchoring and consequently in coercivity increasing.

Boron can be regarded as nonmagnetic inclusion. Indeed, these inclusions can act on the magnetic structure by forming shutting domains which contribute to fix the walls of Bloch and to slow down their displacement and, consequently, an increase in the coercivity.

4. Conclusion

This work is an investigation study on the iron-based thermal sprayed coatings for obtaining a amorphous and nanocrystalline structure using the HVOF spray.

Adjusting the spraying conditions, we were able to obtain amorphous coating from the FeNb powder. However, for the silicon-iron powder, a crystalline deposit was pro-

duced in all cases (microcrystalline and nanocrystalline powders). As suggested, we considered to use boron additives to improve he aptitude of the silicon-iron alloy to form an amorphous phase. In this perspective, we have elaborated first principle calculations to investigate the electronic structure of crystalline FeNb and Fe_3Si. We showed that the introduction of boron impurities into the alloy matrix leads to the lowering of the structural stability, and makes its electronic density of state more comparable to that corresponding to the niobium-iron.

Experiments have showed that the addition of boron in FeSi alloy make possible the aptitude of amorphization. A variation of boron quantity can increase the amorphous phase and consequently the nanocristalline phase.

The development of a theoretical formulation is needed, accounting for the morphology of the nanocrystalline powders, capable of predicting microstructurale evolution during thermal spraying. The formulation and application of robust models to optimize the experimental parameters are also necessary for the thermal spraying of nanocrystalline systems. The application of current available diagnostic tools will ensure the reproducibility of results.

Acknowledgements

We thank J. Kraven and J.Muzard from Nipson Belfort, France, for their technical assistance concerning magnetic measurements.

References

[1] L.L. Shaw, D. Goberman, R. Ren, M. Gell, S. Jiang, Y. Wang, T.D. Xiao, P.R. Strutt, Surf. Coat. Technol. 130 (2000) 1.
[2] R.W. Siegel, Nanostruct. Mater. 4 (1994) 121.
[3] H. Gleiter, Acta Mater. 48 (2000) 1.
[4] D.G. Morris, Materials Science Foundations, vol. 2, Trans. Tech. Publications, Zurich, 1998.
[5] H.G. Jiang, M.L. Lau, E.J. Lavernia, Nanostruct. Mater. 10 (1998) 169.
[6] J. He, M. Ice, E.J. Lavernia, J. Metastable Nanocryst. Mater. 237 (1999) 2.
[7] I. Nishida, Phys. Rev., B 7 (1973) 2710.
[8] I. Yamauchi, T. Okamoto, H. Ohata, I. Ohnaka, J. Alloys Compd. 260 (1997) 162.
[9] N.E. Fenineche, M. Cherigui, A. Kellou, H. Aourag, C. Coddet, in: R. Marple, C. Moreau (Eds.), Proc. Advancing the Science and Applying the Technology, Pub. ASM International, Materials Park, OH, USA, 2003, p. 1409.
[10] N.E. Fenineche, M. Cherigui, H. Aourag, C. Coddet, Mat. Let. 58 (2004) 1797.
[11] M. Cherigui, H.I. Feraoun, N.E. Fenineche, H. Aourag and C. Coddet, Mat. Chem. Phys. (2004) (in press).
[12] Y. Ono, T. Ichirku, I. Ohnaka, I. Yamauchi, J. Alloys Compd. 289 (1999) 220.
[13] J.C. Swartz, R. Kossowsky, J.J. Hahgh, R.F. Krause, J. Appl. Phys. 52 (1981) 3324.
[14] T.V. Larionova, O.V. Tolochko, A.S. Zhuravley, Glass Phys. Chem. 21 (1995) 297.
[15] T.V. Larionova, O.V. Tolochko, N.O. Gonchukova, E.V. Novikov, Glass Phys. Chem. 22 (1996) 248.
[16] T. Egami, Mater. Res. Bull. 13 (1978) 557.
[17] O. Haruyama, N. Asahi, J. Mater. Sci. 26 (1991) 1851.
[18] Y. Takahara, J. Mater. Sci. Eng. (1997) 128.
[19] R.C. O'Handley, J. Megusar, S.W. Sun, Y. Hara, N.J. Grant, J. Appl. Phys. 57 (1985) 3563.
[20] A. Borisova, Y. Borisov, V. Korzhyk, V. Bobrik, A. Ohmori (Eds.), Proceedings of International Thermal Spray Conference, Osaka, Japan, 1995, p. 749.
[21] M. Nakayama, H. Ito, R. Nakamura, M. Toh, A. Ohmori (Eds.), Proceedings of International Thermal Spray Conference Osaka, Japan, 1995, p. 1063.
[22] P.E. Blöchl, O. Jepsen, O.K. Andersen, Phys. Rev. B49 (1994) 16223.
[23] D.D. Koelling, B.N. Harmon, J. Phys. Sol. State Phys. 10 (1977) 3107.
[24] P. Blaha, K. Schwarz, G.K.H. Madsen, D. Kvasnicka, J. Luitz, WIEN2k, An Augmented Plane Wave Plus Local Orbitals Program for Calculating Crystal Properties, Vienna University of Technology, Austria, 2001.
[25] J.P. Perdew, J.A. Chevary, S.H Vosko, K.A. Jackson, M.R. Pederson, D.J. Singh, C. Fiolhais, Phys. Rev., B 46 (1992) 6671.
[26] J.P. Perdew, Y. Wang, Phys. Rev., B 45 (1992) 13244.
[27] R.S. Lima, J. Karthikeyan, C.M. Kay, J. Lindemann, C.C. Berndt, Thin Solid Films 416 (2002) 129.
[28] L.K. Varga, F. Mazaleyrat, J. Kovac, A. Kàkay, Mater. Sci. Eng. A304-306 (2001) 946.
[29] M. Abdellaoui, C. Djega-Mariadassou, E. Gaffet, J. Alloys Comp. 259 (1997) 241.
[30] E.F. Kneller, in: A.E. Berkowitz, E. Kneller (Eds.), Mag. Metall., Academic Press, New York, 1969, p. 365.
[31] R.M. Bozorth, Ferromagnetism, England, 1951, p. 77.
[32] T. Zhou, J. Zhang, J. Xu, Z. Yu, G. Gu, D. Wang, H. Huang, Y. Du, J. Wang, Y. Jiang, J. Mag. Mat. 164 (1996) 219.
[33] P. Jacubovics, Magn. Magn. Mater., The Institute of Metals, London, 1987, p. 71.